

Supporting Information for:

**Oxygen Deficient and Nitrogen Doped MnO₂ Nanowire–Reduced
Graphene Oxide–Cellulose Nanofibril Aerogel Electrodes for High-
Performance Asymmetric Supercapacitors**

Qifeng Zheng^{a,b}, Ruosen Xie^{a,b}, Liming Fang^{b,c}, Zhiyong Cai^d, Zhenqiang Ma^{a,e}, and
Shaoqin Gong^{a,b,f,g*}

^a *Department of Material Science and Engineering, University of Wisconsin–Madison, WI 53706, USA.*

^b *Wisconsin Institute for Discovery, University of Wisconsin–Madison, WI 53715, USA*

^c *School of Materials Science and Engineering, South China University of Technology, Guangzhou 510641, PR China*

^d *Forest Product Laboratory, USDA, Madison, WI 53726, USA*

^e *Department of Electrical Engineering, University of Wisconsin–Madison, WI 53706, USA*

^f *Department of Biomedical Engineering, University of Wisconsin–Madison, WI 53706, USA*

^g *Department of Chemistry, University of Wisconsin–Madison, WI 53706, USA*

**Corresponding Author; Email: shaoqingong@wisc.edu; Tel: +01 6083164311.*

Supplementary Experimental Details

Materials: 2,2,6,6-tetramethyl-1-piperidinyloxy (TEMPO, 98 wt.%), potassium permanganate (99 wt.%), hydrogen peroxide solution (30 wt.%), natural graphite flakes (100 mesh), sulfuric acid (98 wt.%), poly(vinyl alcohol) (PVA, M_w : 89 kDa–98 kDa), $MnSO_4 \cdot H_2O$, $KClO_3$, Na_2SO_4 , CH_3COOK , and CH_3COOH were purchased from Sigma–Aldrich. Molybdenum powder (99.5 wt.%, ~170 mesh) and hydrazine monohydrate (98 wt.%) were obtained from Alfa Aesar. Sodium chlorite, sodium hypochlorite solution, sodium bromide, phosphoric acid, and other chemicals were of laboratory grade (Fisher Scientific, USA) and used without further purification.

Preparation of Cellulose Nanofibrils (CNFs): A commercially supplied, fully bleached eucalyptus Kraft pulp was used to prepare the CNFs by TEMPO-oxidation as previously reported.^{1, 2} Briefly, fully bleached eucalyptus fibers were oxidized with sodium hypochlorite using TEMPO as a catalyst at a temperature of 60 °C for 48 h. The fibers were then thoroughly washed and refined in a disk refiner with a gap of approximately 200 μm . The coarse fibers were separated by centrifuging at 12,000 G, and the fine CNF dispersion was then concentrated using ultrafiltration. A final refining step was performed in which the nanofiber dispersion was passed through an M-110EH-30 microfluidizer (Microfluidics, Newton, MA) once with 200 μm and 87 μm chambers in series. The resulting CNF suspension with a concentration of 0.90% was stored at 4 °C without any treatment before future utilization.

Preparation of Graphene Oxide (GO): Graphene oxide (GO) was prepared from purified natural graphite powder using an improved Hummer's method reported by Marcano.^{2, 3} To be specific, graphite flakes (2.0 g) and KMnO₄ (12.0 g) were slowly added into a mixture of concentrated H₂SO₄/H₃PO₄ (180 ml:20 ml) and then heated at 50 °C for 12 h. Afterward, the mixture was cooled to room temperature and then poured into a mixture of ice (~200 ml) with H₂O₂ solution (2 ml, 30 wt.%). The mixture was centrifuged at 10,000 rpm for 15 min, and the supernatant was decanted. The remaining solid material was then washed in succession with water, 30% HCl, ethanol, and water. The remaining solid was further purified by dialysis against DI water until the pH of the solution was above 6. The solution after dialysis was freeze-dried to obtain the GO powder (3.6 g).

Preparation of Ultralong Molybdenum Trioxide Nanowires (MoO₃): The ultralong molybdenum trioxide was prepared using a modified hydrothermal method as previously reported.⁴ Briefly, molybdenum powder (2.0 g) was dispersed in deionized water (15 mL) via sonication. Afterward, H₂O₂ (20 mL, 30 wt.%) was added dropwise and the solution was continuously stirred for 30 min to react thoroughly. The resulting mixture was transferred to a 50 mL Teflon-lined stainless steel autoclave, which was then heated at 200 °C for 5 days. The precipitate was then filtered and washed with water and ethanol several times until the solution became clear. The solid material was freeze-dried to obtain the MoO₃ nanowires (2.42 g).

Calculations: The electrochemical parameters were calculated as follows.^{5,6}

For the three-electrode system, the specific capacitances of the electrodes based on the mass or area or volume were calculated from their galvanostatic charge–discharge curves at different current densities using Equations (S1), (S2), and (S3), respectively,

$$C_{M, electrode} = \frac{I \times \Delta t}{M_1 \times \Delta V} \quad (S1)$$

$$C_{A, electrode} = \frac{I \times \Delta t}{S_1 \times \Delta V} \quad (S2)$$

$$C_{V, electrode} = \frac{I \times \Delta t}{V_1 \times \Delta V} \quad (S3)$$

where I is the discharge current and Δt is the discharge time of the galvanostatic charge/discharge curves, and ΔV is the operating voltage window from the discharge curve excluding the IR drop. Parameters M_1 , S_1 , and V_1 are the active working weight, area, and volume of the working electrodes in the three-electrode system, respectively.

For the two-electrode liquid and the all-solid-state asymmetric supercapacitors (ASCs), the gravimetric ($C_{m, device}$, in F/g), areal ($C_{A, device}$, in mF/cm²), and volumetric ($C_{V, device}$, in F/cm³) capacitance of the ASC devices were calculated from their galvanostatic charge–discharge curves at different current densities using the following equations.

$$C_{M,device} = \frac{I \times \Delta t}{M_2 \times \Delta V} \quad (S4)$$

$$C_{A, device} = \frac{I \times \Delta t}{S_2 \times \Delta V} \quad (S5)$$

$$C_{V, device} = \frac{I \times \Delta t}{V_2 \times \Delta V} \quad (S6)$$

The energy density and power density of the two-electrode supercapacitors were calculated according to Equations (S10) and (S11), respectively,

$$E_{device} = \frac{C_{device} \times (\Delta V)^2}{2 \times 3600} \quad (S10)$$

$$P_{device} = \frac{E_{device} \times 3600}{\Delta t} \quad (S11)$$

where I is the discharge current, Δt is the discharge time of the galvanostatic charge/discharge curves, and ΔV is the operating voltage window from the discharge curve excluding the IR drop. Parameter M_2 is the sum weight of positive and negative electrodes used in the ASC devices. S and V are the area and volume of ASC devices, respectively.

The mass loading of the active materials in the positive and negative electrodes were calculated to be 6.02mg/cm² and 5.10 mg/cm², respectively. The calculation details are as follows:

During the preparation steps, we kept the CNFs—the non-electrochemically active materials—at the same percentage (i.e., 20 wt.%), and the MnO₂ and GO in the MnO₂/GO/CNF aerogels were set at 40 wt.% and 40 wt.%, respectively. Before

hydrazine vapor treatment, the $\text{MnO}_2/\text{GO}/\text{CNF}$ aerogel has a weight of 200 mg, an areal density of $8.13 \text{ mg}/\text{cm}^2$ (Figure 2d), corresponding to a mass loading of $6.50 \text{ mg}/\text{cm}^2$ of the active materials (i.e., MnO_2 and GO). After the hydrazine vapor treatment, the weight was decreased to 188 mg for the $\text{MnO}_x\text{N}_y/\text{RGO}/\text{CNF}$ aerogel. Since the hydrazine vapor treatment was conducted at $140 \text{ }^\circ\text{C}$, the CNF should be stable at this temperature, thus we assume that the weight of the CNF remained the same after treatment. Therefore, the weight of the active materials (i.e., MnO_xN_y and RGO) in the $\text{MnO}_x\text{N}_y/\text{RGO}/\text{CNF}$ aerogel was calculated to be 148 mg, corresponding to a mass loading of $6.02 \text{ mg}/\text{cm}^2$ of the real active materials (i.e., MnO_xN_y and RGO). The same correction was also applied for the $\text{MoO}_x\text{N}_y/\text{RGO}/\text{CNF}$ and RGO/CNF aerogels, which showed a corrected active materials loading of $5.10 \text{ mg}/\text{cm}^2$ and $5.85 \text{ mg}/\text{cm}^2$, respectively. All the data and figures in the manuscript were calculated and plotted based on the mass loading contents of the active materials calculated after the hydrazine vapor treatment.

For the ASC devices, the area made accessible to the electrolyte was 2.0 cm^2 , corresponding to a total mass of 22.24 mg of the active materials (MnO_xN_y , MoO_xN_y , and RGO).

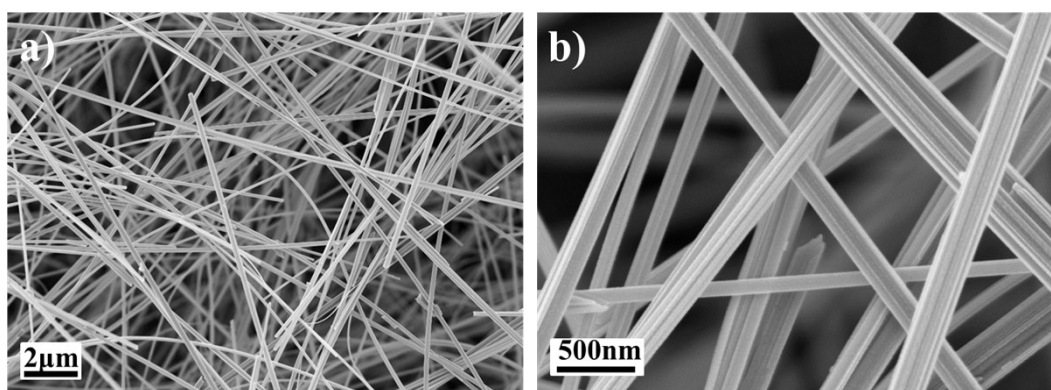


Figure S1. (a, b) SEM images of the ultra-long MnO₂ nanowires.

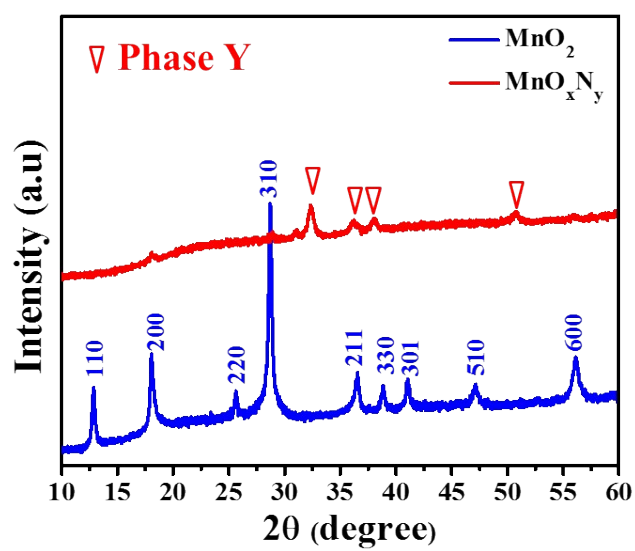


Figure S2. XRD patterns of the MnO₂ and MnO_xN_y nanowires.

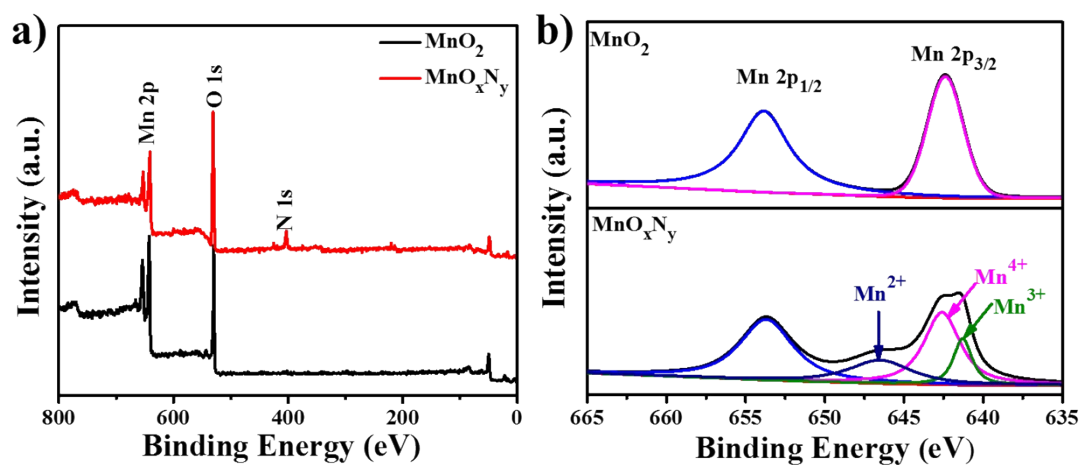


Figure S3. (a) XPS survey spectra and (b) high-resolution Mn2p XPS spectra of the MnO_2 and MnO_xN_y nanowires.

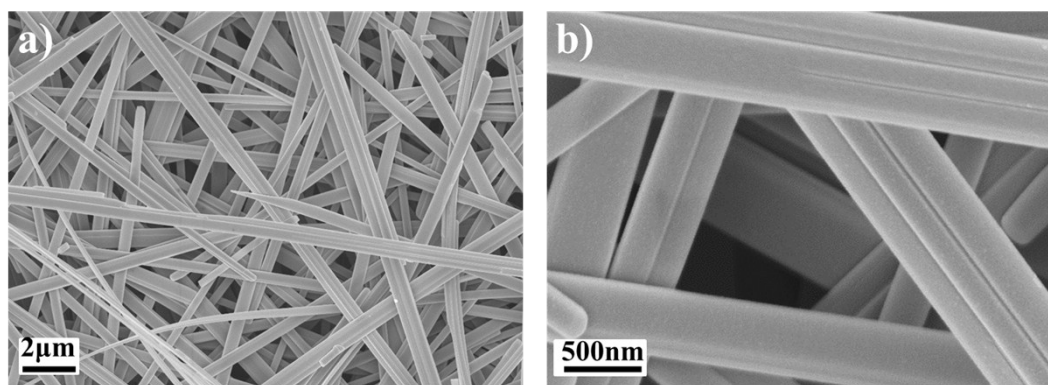


Figure S4. (a, b) SEM images of the ultra-long MoO_3 nanowires.

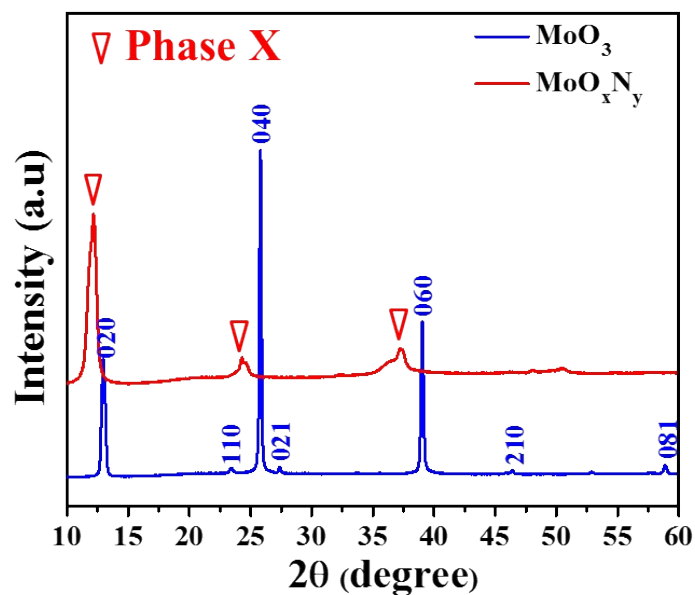


Figure S5. XRD patterns of the MoO_3 and MoO_xN_y nanowires.

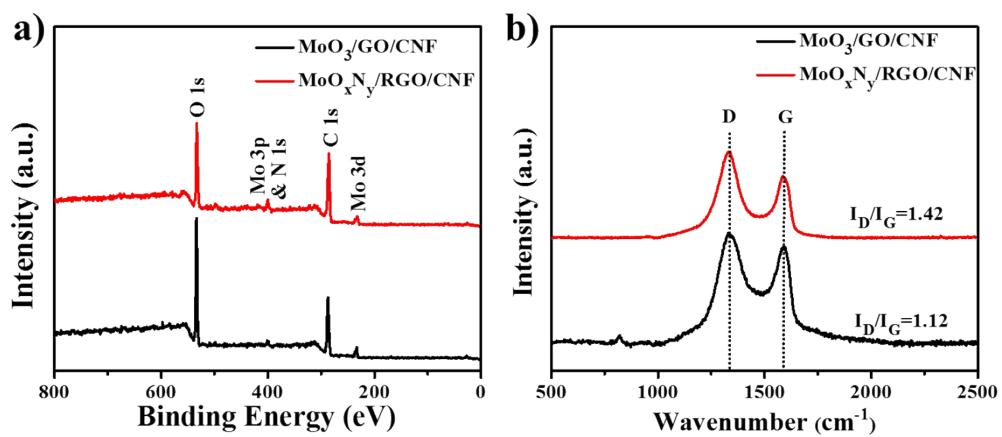


Figure S6. (a) XPS survey spectra and (b) Raman spectra of the $\text{MoO}_3/\text{GO}/\text{CNF}$ and $\text{MoO}_x\text{N}_y/\text{RGO}/\text{CNF}$ aerogels.

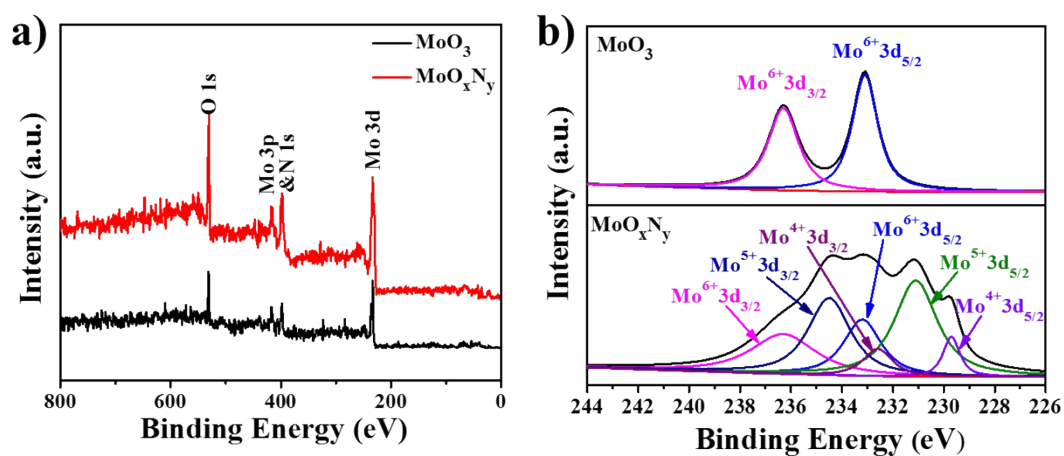


Figure S7. (a) XPS survey spectra and (b) high-resolution Mo3d XPS spectra of the MoO_3 and MoO_xN_y nanowires.

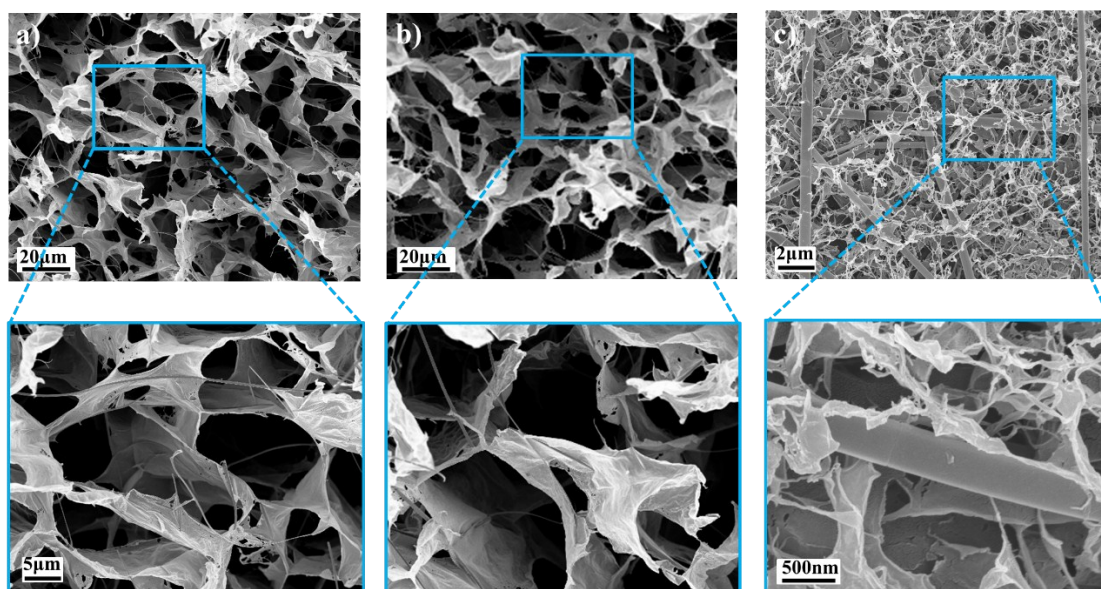


Figure S8. SEM images of various aerogels: (a) the $\text{MoO}_3/\text{GO}/\text{CNF}$ aerogel, (b) the $\text{MoO}_x\text{N}_y/\text{RGO}/\text{CNF}$ aerogel, and (c) the compressed $\text{MoO}_x\text{N}_y/\text{RGO}/\text{CNF}$ aerogel film.

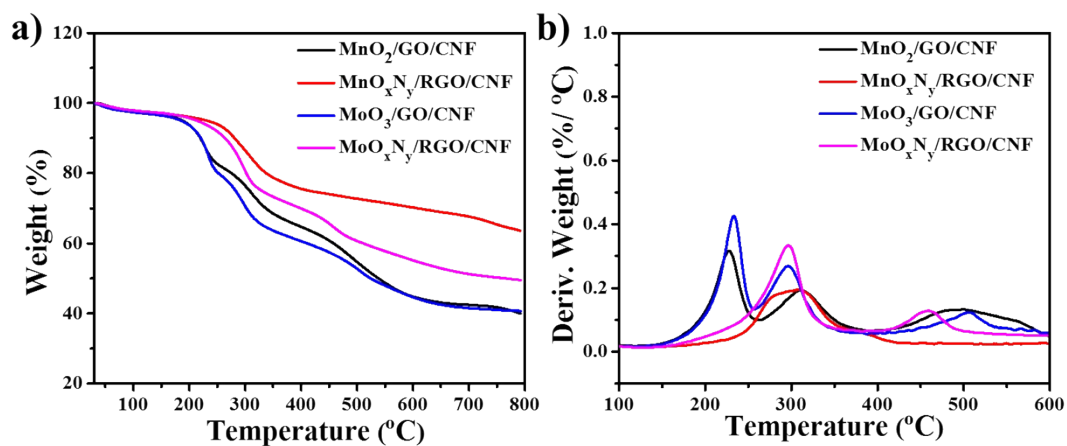


Figure S9. (a) TGA curves and (b) DTG curves of the $\text{MnO}_2/\text{GO}/\text{CNF}$, $\text{MnO}_x\text{N}_y/\text{RGO}/\text{CNF}$, $\text{MoO}_3/\text{GO}/\text{CNF}$, and $\text{MoO}_x\text{N}_y/\text{RGO}/\text{CNF}$ aerogels

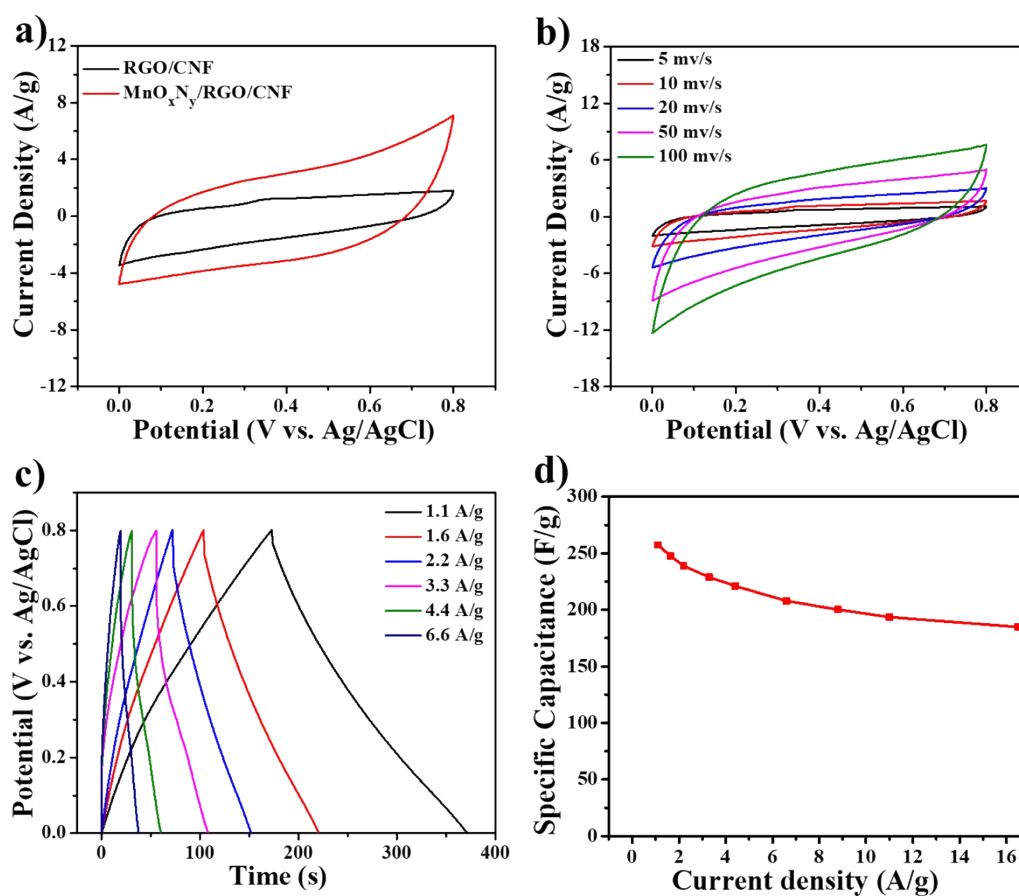


Figure S10. (a) Typical CV curves of the RGO/CNF and MnO_xN_y/RGO/CNF aerogel film electrodes at a scan rate of 10 mV/s. (b) Typical CV curves of the RGO/CNF aerogel film electrodes at different scan rates. (c) Galvanostatic charge–discharge curves of the RGO/CNF aerogel film electrodes at different current densities. (d) Specific capacitance of the RGO/CNF aerogel film electrodes as a function of current density.

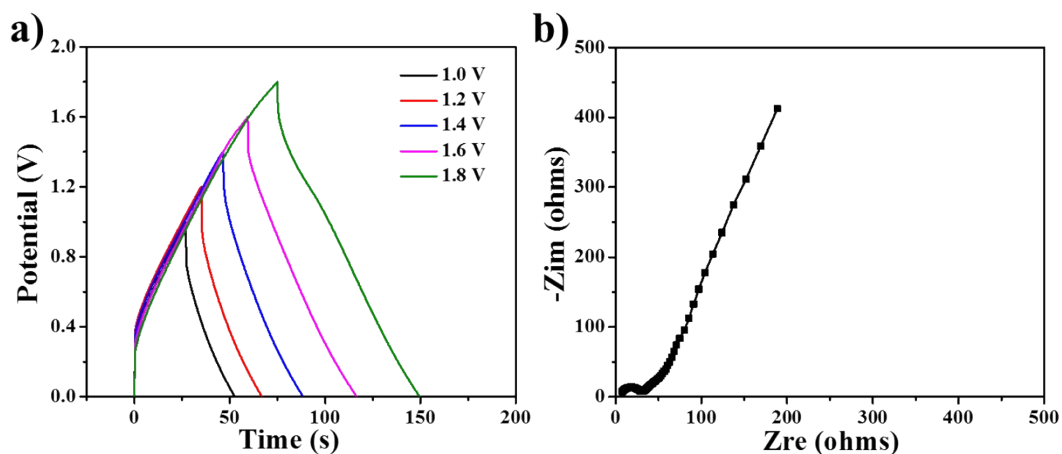


Figure S11. (a) Galvanostatic charge–discharge curves of the liquid ASC device under different potential windows at a current density of 2 A/g. (b) Nyquist impedance plots of the liquid ACS device.

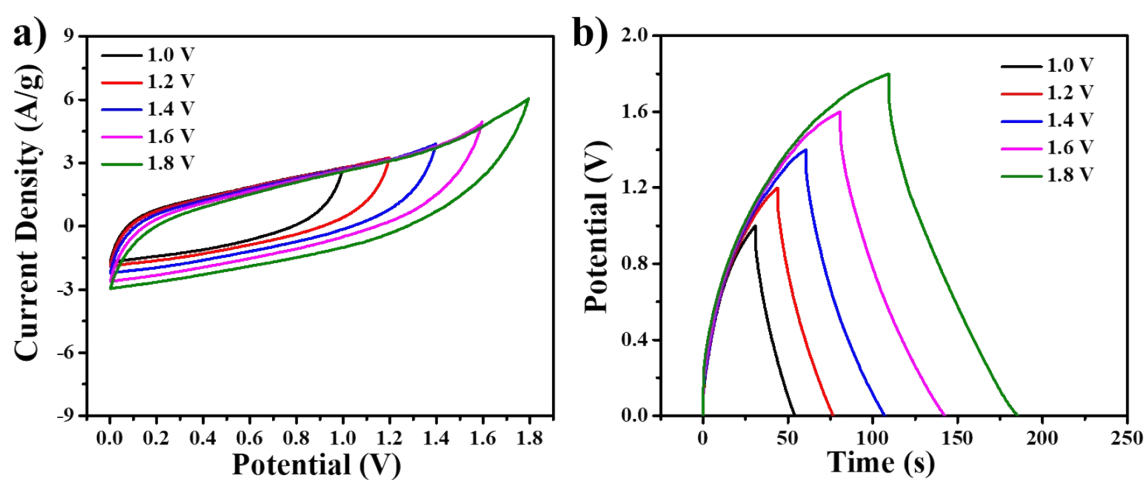


Figure S12. (a) CV curves of the solid-state ASC device under different potential windows at a scan rate of 20 mV/s. (b) Galvanostatic charge–discharge curves of the solid-state ASC device under different potential windows at a current density of 2 A/g.

Supplementary Video S1: One single ASC device can light the LED very well.

References:

1. A. Javadi, Q. Zheng, F. Payen, A. Javadi, Y. Altin, Z. Cai, R. Sabo and S. Gong, *Acs Appl Mater Inter*, 2013, **5**, 5969-5975.
2. Q. Zheng, Z. Cai, Z. Ma and S. Gong, *Acs Appl Mater Inter*, 2015, **7**, 3263-3271.
3. D. C. Marcano, D. V. Kosynkin, J. M. Berlin, A. Sinitskii, Z. Sun, A. Slesarev, L. B. Alemany, W. Lu and J. M. Tour, *ACS Nano*, 2010, **4**, 4806-4814.
4. C.-H. Liu, Y.-C. Chang, T. B. Norris and Z. Zhong, *Nat Nano*, 2014, **9**, 273-278.
5. H. Wang, C. Xu, Y. Chen and Y. Wang, *Energy Storage Materials*, 2017, **8**, 127-133.
6. Q. Zheng, A. Kvit, Z. Cai, Z. Ma and S. Gong, *Journal of Materials Chemistry A*, 2017, **5**, 12528-12541.